Available online at www.eccomasproceedia.org
Eccomas Proceedia COMPDYN (2017) 2996-3010

ECCOMAS
Proceedia

COMPDYN 2017
6th ECCOMAS Thematic Conference on
Computational Methods in Structural Dynamics and Earthquake Engineering
M. Papadrakakis, M. Fragiadakis (eds.)
Rhodes Island, Greece, 15–17 June 2017

ENERGY DISSIPATION INVOLVED IN THE OUT-OF-PLANE RESPONSE OF UNREINFORCED MASONRY WALLS

U. Tomassetti[1], F. Graziotti[1,2], A. Penna[1,2], and G. Magenes[1,2]

[1] Dept. of Civil Engineering and Architecture, University of Pavia,
via Ferrata 3, 27100 Pavia, Italy.
umberto.tomassetti01@univeristadipavia.it

[2] European Centre for Training and Research in Earthquake Engineering,
via Ferrata 1, 27100 Pavia, Italy.
francesco.graziotti@unipv.it, andrea.penna@unipv.it, guido.magenes@unipv.it

Keywords: URM, out-of-plane, rocking, one-way bending, coefficient of restitution, elastic viscous damping ratio.

Abstract. *The assessment of the out-of-plane response of masonry has been largely investigated in literature assuming walls responding as rigid blocks or assemblies of rigid bodies. Several studies developed numerical integration of single-degree-of-freedom and multi-degree of freedom systems for the simulation of the OOP dynamic rocking response of simple mechanisms. Modelling the energy dissipation involved in such mechanisms is extremely important to capture the dependence of the damping phenomenon with the system frequency.*

Some studies, recurring to the classical hypothesis of the impulsive dynamics, simulated the energy dissipation by means of the coefficient of restitution assuming as the overall reduction of energy were concentrated at the instant of the impact. In other works, the damping force has been modelled as a velocity dependent acting force through a constant, variable or stiffness proportional damping ratio.

The two damping models are compared highlighting advantages and shortcomings of each system. This paper proposes a numerical formulation for the direct equivalence of the two damping approaches for simple OOP one-way bending mechanisms assuming as force-displacement relationship nonlinear elastic tri-linear curves.

Peer-review under responsibility of the organizing committee of COMPDYN 2017.
doi: 10.7712/120117.5622.18454

1 INTRODUCTION

The high seismic vulnerability of unreinforced masonry (URM) structures has been highlighted in many studies in the literature [1-3]. The out-of-plane (OOP) behaviour of URM structures subjected to ground motion excitations has been extensively investigated by referring to the rocking dynamic of semi-rigid wall segments, characterised by consistent rotations, that impact each other. Such interpretation, confirmed by several experimental campaigns, could be considered acceptable under specific hypothesis and in case the masonry quality is good enough to ensure the formation of such mechanism. The understanding of this complex dynamic behaviour is essential in assessing the seismic performance of existing structures, for which an accurate prediction of displacement capacity and demand is essential in both safety verifications and risk analyses.

Housner [4] with a pioneer study derived a single degree of freedom (SDOF) equation of motion for dynamic response of slender rigid blocks (inverted pendulum structures) that could easily represent the one-way OOP response of a parapet wall (PW). Several studies [5-6], assuming that both end supports of the wall move simultaneously, derived SDOF equation of motion for the one-way vertical spanning strip walls (VSSW) displacing as an assembly of two rigid bodies. Dejong and Dimitrakopoulos [7] as well as Restrepo [8] extended the solution to include equivalent SDOF systems governing the dynamic behaviour of complex multi-block systems responding in rocking.

Makris and Konstantinidis [9] highlighted that the classical linear oscillator (regular pendulum) often adopted to analyse the OOP behaviour of masonry sub-structures, and the rocking block represent two fundamentally different dynamical systems. Rocking structures, indeed, do not have a fundamental period of vibration, the responding frequency is, hence, oscillation amplitude dependent [4-5]. Further differences between these two systems are also represented by restoring mechanisms, stiffness and characteristics of the damping phenomena. Therefore, equivalent stiffness methods based on the adoption of classical response spectra [10] cannot sufficiently predict the response of rocking structures. Makris and Konstantinidis proposed the derivation of rocking spectra as a more adequate approach to characterising the earthquake input. For these reasons, the solution proposed by several researchers to the challenging problem of assessing the OOP performance of URM structures has been to directly integrate the rocking equation of motion to reproduce their dynamic responses.

Recognising that the URM wall segments do not have infinite stiffness, researchers proposed bi-linear [11], tri-linear [6] and four-branch [12] non-linear elastic curves to model the force-displacement (F-u) relationship.

The energy dissipation in elastic non-linear systems (i.e. rocking structures) is of major importance to successfully simulate their dynamic behaviour, capturing the dependence of the damping phenomenon with the system frequency. Some studies, building off the classical hypothesis of the impulse dynamics, simulated the energy dissipation involved in such mechanisms by means of the coefficient of restitution assuming that the overall reduction of energy was concentrated at the instant of the impact [4-5]. In other works, the damping force has been modelled as a velocity dependent force through a constant [10] and variable (with cycle-to-cycle iterations) damping ratio [13]. The effectiveness of damping models acting on the system secant stiffness with a constant or linear damping ratio-frequency (ξ- ω) relationship is also investigated [14].

The present study proposes a correlation between these different damping systems: elastic viscous dampers and coefficient of restitution focusing on the response of VSSW systems. The second section introduces the SDOF rigid body equation of motion. Section 3 reviews the tri-linear idealisation commonly used to simulate the static OOP force-displacement relationship

of a VSSW. The energy dissipation involved in this phenomenon is discussed in section 4 introducing both coefficient of restitution and velocity dependent damping force systems. Section 5 presents the numerical model developed from the present study. The results of the proposed equivalence and their experimental validation is discussed in section 6 and 7.

2 RIGID BODY SDOF EQUATION OF MOTION

Figure 1 shows the VSSW deformed shape responding in pure rocking behaviour characterised by the formation of the classical pivot interfaces at the wall top, bottom and mid-height. The resulting top and bottom rigid bodies rotate around such pivot (A'-B-C' in Figure 1) points impacting each other every time the system passes through mid-height horizontal rest-condition displacement (u=0 in Figure 1). α_2 and α_1 are geometric angles defining the slenderness of the two bodies; W_2 and W_1 represent the weight of the top and bottom bodies applied at the bodies centre of mass, O is the overburden vertical force applied with eccentricity e, t the thickness of the wall. θ_2 and θ_1 are the top and bottom body rotations equal to u/h_2 and u/h_1 respectively.

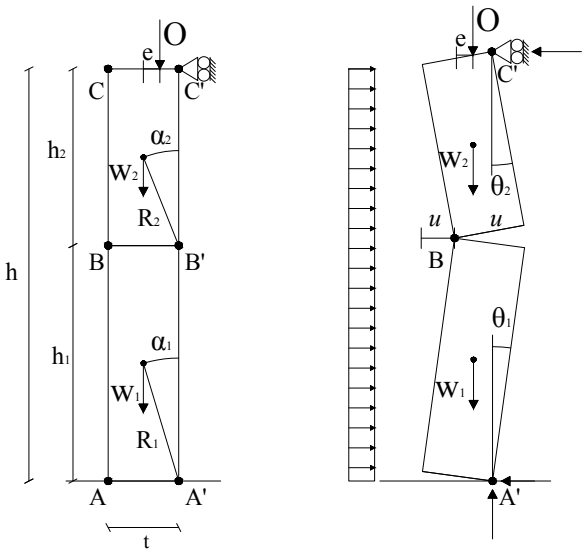

Figure 1: VSSW responding in Rocking behaviour: geometry at rest and deformed shape.

The equation of motion of this system responding in rocking can be derived directly from Lagrange's equation of motion. Under the hypothesis of no sliding, no bouncing effect, slender blocks (that allows us to linearize the equation) and assuming both supports moving simultaneously, similarly to Derakhshan *et al.* [15], the generic undamped SDOF equation of motion of a VSSW system can be written as follows:

$$m_{eff} \cdot \ddot{u}(t) + f_{bi}\,(u,t) = -\lambda \cdot m_{eff} \cdot \ddot{u}_g(t) \tag{1}$$

where u represents the horizontal displacement associated to the wall mid-hinge location (shown in Figure 1), m_{eff} is the effective mass of the system affected by the rotational moment of inertia of the two blocks (equation 2), f_{bi} (u, t) is the bi-linear rigid restoring force relationship (equation 3) assuming a uniformly distributed lateral face load (considering uniform thickness and density along the wall height); λ (equation 4) is the parameter that allow to mobilise the entire mass (m_1+m_2) in the excitation term (right side of the equation) with the ground acceleration ($\ddot{u}_g(t)$).

$$m_{eff} = \frac{2}{3}(m_1 + m_2) \tag{2}$$

$$f_{bi}(u,t) = \frac{2}{h_1} \cdot W \cdot (t - u(t)) + \frac{h}{h_1 \cdot h_2} \cdot O \cdot (t + 2e - u(t)) + \frac{2}{h_1} \cdot O \cdot (t - 2e) \quad (3)$$

$$\lambda = \frac{3}{2} \quad (4)$$

The resulting equation of motion is equivalent to those proposed by Sorrentino et al. [5], DeJong & Dimitrakopoulos [7]. The aforementioned studies described the rocking phenomena as function of the rotation of the lower body. Sorrentino *et al.* [5] have shown as the system frequency parameter considering h_1/h ratios different from 0.5 may slightly affect m_{eff} and λ. Experimental evidences have shown as this ratio could be addressed between 0.5 and 0.7 [16-17].

3 FORCE-DISPLACEMENT RELATIONSHIP

Before undergoing non-linear rocking behaviour through the formation of the classical pivot interfaces, URM walls are characterised by a linear response controlled by the masonry flexural stiffness till the attainment of the cracking force. Neglecting the wall un-cracked response may lead to a significant underestimation of the lateral capacity, especially for slender and slightly loaded walls, and an overestimation of the OOP displacement demand [6, 18].

The bi-linear curve relies on the assumption of wall responding as an assembly of two rigid bodies with an infinite initial stiffness and strength, representing an upper bound of the real OOP static resistance of a VSSW. The bi-linear curve could be identified by F_0 and u_{ins} the defined according to the equations:

$$F_0 = \frac{2}{h_1}(W + O) \cdot t + \frac{O}{h - h_1}(t + 2e) \quad (5)$$

$$u_{ins} = \frac{2/h_1\,(W + O)t + O \cdot (t + 2 \cdot e)/(h - h_1)}{2/h_1\,(W + O) + 2O/(h - h_1)} \quad (6)$$

K_0 represents the negative stiffness of the system. The experimental *F-u* relationship of a VSSW could be more realistically represented by a tri-linear curve built on the rigid body bi-linear idealisation. Figure 2 illustrates the both the rigid-bilinear curve and the tri-linear relationships implemented in the model. The key parameters of the tri-linear relationship are u_1 ($=a_1 \cdot u_{ins}$) controlling the wall's initial cracked stiffness, and F_y ($= b_1 \cdot F_0$) identifying a force plateau; the idealisations proposed in literature beyond u_2, generally located along the bi-linear curve ($u_2 = u_{ins} - F_y/K_0$), drops to zero in some cases matching the bi-linear idealisation ($u_3 = u_{ins}$), in some other cases with an higher negative stiffness ($u_3 = a_3 \cdot u_{ins}$) taking into account the masonry compressive strength and the physical dimension of the hinges [19]. In this latter case, it may also be represented by a backward translation (with negative stiffness equal to K_0) of the last tri-linear branch causing a reduction of the u_2 value.

The values for a_1, a_3 and b_1 are strongly affected by aspects such as wall thickness, acting vertical overburden force and masonry mechanical properties [19]. Doherty [6] identified three stages of degradation: new, moderate and severe corresponding to b_1 values of 0.72, 0.60 and 0.50 and a_1 values of 0.06, 0.13 and 0.20, respectively. Other researchers later suggested a_1 values of 0.04 [18] and 0.05 [5] based on both experimental results of air-bag quasi-static tests and successful numerical modelling of the dynamic behaviour of VSSW systems. Derakhshan *et al.* [18] showed as a_2 value of 0.25 represents an upper bound level for this parameter. Their experimental work also suggested that the average ratio between the maximum lateral force resistance and the F_0 rigid force for two-leaf and three-leaf walls was around 0.81 suggesting b_1 values around 0.75 (1- a_2) [15]. A refined work on the characterisation of the *F-u* relationship of can be found in [19].

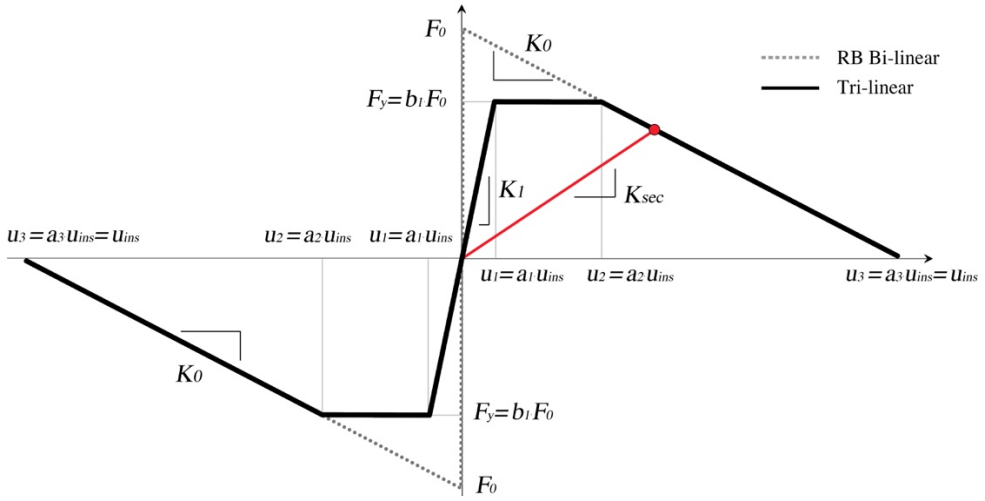

Figure 2: *F-u* relationship implemented: tri-linear configuration built on the bi-linear rigid body idealisation.

4 ENERGY DISSIPATION IN ROCKING STRUCTURES

The overall damping force acting in URM panels or assemblies responding in OOP rocking is given primarily by the energy dissipated through the impact of the wall during rocking in addition to a small contribution from the hysteretic energy dissipation, which both need to be considered in the model. A common approach, relying on the classical hypothesis of the impulse dynamics, is simulating the energy dissipation involved in such mechanisms through a coefficient of restitution [4-5, 20]. Another option is adopting an equivalent viscous damping approach defining a velocity dependent damping force through a constant, variable (with cycle-to-cycle iterations) and stiffness proportional damping ratio. The iterative procedure introduced by Doherty [6] and Lam *et al.* [13] consisted in evaluating the damping associated with each half-response cycle according to a calibration of Rayleigh damping against dynamic experimental ξ- ω data. This study will be focused only on non-iterative damping force model and systems adopting the coefficient of restitution. Both of these approaches are discussed in the following subsections.

4.1 The coefficient of restitution

Aslam *et al.* [21] defined the restitution coefficient as the direct ratio e_{an} between angular velocities after ($\dot{\theta}_{n+1}$) and before ($\dot{\theta}_n$) the n^{th} impact. Assuming an infinitesimal impact duration hence instant velocity variation, no displacement during impact and imposing the conservation of angular momentum around the rotational hinge by equating the angular momentum after and before the impact, a theoretical coefficient of restitution can be derived for a VSSW system as the ratio between the angular velocities after and before the impact [5]:

$$e_{an} = \frac{m_1 {R_1}^2 + I_{CM,1} - I_{CM,2}\frac{\tan\alpha_2}{\tan\alpha_1} - 2m_1 {R_1}^2 \sin^2\alpha_1 + m_2 {R_1}^2\left[2 + \frac{\sin\alpha_1\cos\alpha_1}{\tan\alpha_2} - \sin^2\alpha_1\left(4 + \frac{\tan\alpha_2}{\tan\alpha_1}\right)\right]}{m_1 {R_1}^2 + I_{CM,1} - I_{CM,2}\frac{\tan\alpha_2}{\tan\alpha_1} + m_2 {R_1}^2\left[2 + \sin\alpha_1\cos\alpha_1\left(\frac{1}{\tan\alpha_2} + \tan\alpha_2\right)\right]} \quad (7)$$

where $I_{CM,1}$ and $I_{CM,2}$ are the polar moment of inertia around the two blocks centre of mass for a VSSW system. Note that the coefficient of restitution depends on the system slenderness, the squatter the wall (α_1) the higher is the energy dissipation (lower e_{an}). The coefficient of restitution experimentally observed is lower than e_{an}, and Sorrentino therefore proposed an experimental coefficient of restitution e_{exp} that is $0.90 \cdot e_{an}$ for a VSSW [22]. Graziotti *et al.*

observed for a VSSW system values of coefficient of restitution between 0.90 and 0.84 (specimen slenderness around 27) [17]. Adopting the aforementioned definition, the coefficient of restitution acts in the numerical model by reducing the system velocity at each *n-th* impact (every time the horizontal displacement *u* passes through the null displacement) as follows:

$$\dot{u}_{n+1}(t + dt) = e_{exp} \cdot \dot{u}_n(t) \tag{8}$$

4.2 The Equivalent Viscous Damping

The energy dissipation can also be modelled through an equivalent viscous damping force. A classical damping model with a constant damping coefficient (CDC), assuming a constant damping ratio (ξ) acting on the system initial stiffness (ω_1), is commonly adopted to simulate the dynamic response of rocking systems [10]. Moreover, two other damping systems have also been investigated and compared in order to capture the dependence of the damping phenomenon on the oscillation amplitude and on the current frequency of vibration of the system. Both damping models act on the instantaneous secant frequency $\omega(t)$ defined by the instantaneous secant stiffness $K_{sec}(t)$ of the system (slope of the red line in Figure 2) and presented in equation 9:

$$\omega(t) = \sqrt{\frac{K_{sec}(t)}{m_{eff}}} \tag{9}$$

The first one of the two associates a constant damping ratio through all the system frequencies, whereas the second one assumes a stiffness proportional term (ξ-ω linear relationship) identified by the damping ratio (ξ_{in}) corresponding to the frequency of the first branch of the tri-linear relationship (ω_1 or F_1). The damping coefficient of the three damping models: CDC, constant damping ratio (CDR) and stiffness proportional damping ratio (SDR), is defined by equations 10, 11, 12 respectively:

$$C_{CDC} = 2 \cdot m_{eff} \cdot \omega_1 \cdot \xi \tag{10}$$

$$C_{CDR}(t) \cdot= 2 \cdot m_{eff} \cdot \omega(t) \cdot \xi \tag{11}$$

$$C_{SDR}(t) \cdot= 2 \cdot m_{eff} \cdot \omega(t) \cdot \xi(\omega(t)) \tag{12}$$

Figure 3 compares the three damping models in terms of damping ratio - frequency (ξ- ω) relationship and distribution of the damping forces through the non-dimensional oscillation amplitude in matched rocking free vibration decays of a VSSW. Both CDR and SDR models, acting on the secant frequency, tend to concentrate the energy dissipation around the zero-oscillations amplitude, which correspond to the impact region, acting in a similar fashion of a coefficient of restitution. The area within the loops in Figure 3 representing the dissipated energy is the same for each damping model.

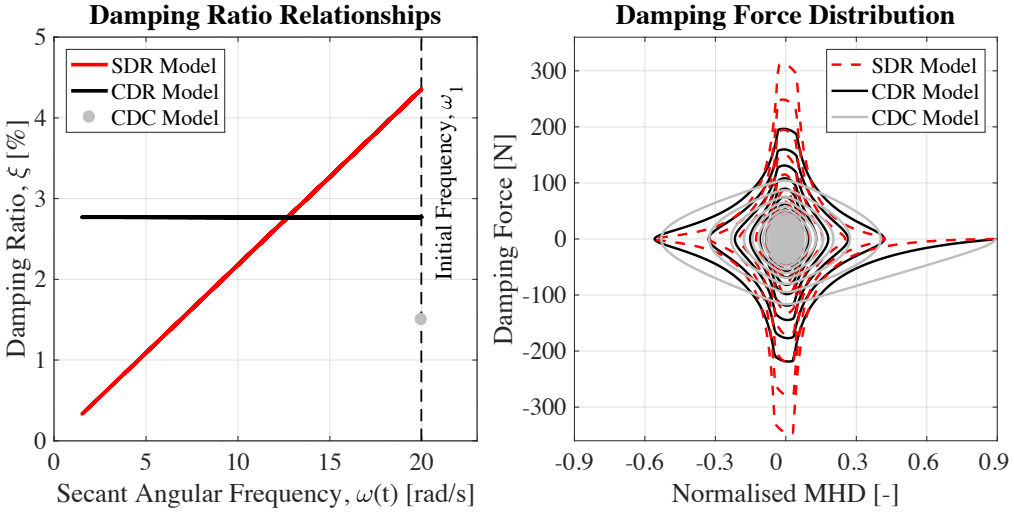

Figure 3: Left side: comparison between ξ- ω relationships of the three models. Independently from the actual or secant frequency of the system the CDC damp the system proportionally the initial angular frequency. CDR and SDR damping models associate to the current secant frequency a damping ratio according to a constant or a linear (defined by the ξ value assigned to ω_1) law; Right side: distribution of the damping force through the normalised oscillation amplitude of the three damping models: CDC, CDR, SDR.

4.3 An Equivalence between the Different Damping Systems

An equivalence between such different damping systems can be carried out by equating the energy losses provided by the different sources of damping. Generally, the coefficient of restitution, imposing a drop in the velocity at each impact, reduces the system kinetic energy. Considering half cycle of displacement between two successive response peaks (positive peak u_p^+ and negative peak u_p^-) of a system in free vibration phase, the energy loss due to impact, passing through displacement level equal to zero is given by the difference of kinetic energies after and before the collision:

$$\Delta T = T^+ - T^- = \frac{1}{2}\sum_{1}^{i} I_{CMi} \cdot \dot{\theta}_i^{+2} + m_i \cdot v_{CMi}^{+\,2} - \frac{1}{2}\sum_{1}^{i} I_{CMi} \cdot \dot{\theta}_i^{-2} + m_i \cdot v_{CMi}^{-\,2} \tag{13}$$

where $\dot{\theta}_i^+$ and $\dot{\theta}_i^-$ are the two bodies angular velocities after and before the impact defined by the rotations according to Figure 1, whereas v_{CMi}^+ and v_{CMi}^- are the centre of mass velocities vectors composed by the two horizontal and vertical components (being the problem defined in 2D): $\dot{u}$ and $\dot{z}$.

The loss of energy due to an acting viscous damping force can be computed as the work done by the damping force in the considered response and time interval; this yields in the integral of equation 6:

$$\Delta E = \int_{u_p^+}^{u_p^-} \begin{matrix} C_{CDC} \\ C_{CDR}(t) \\ C_{SDR}(t) \end{matrix} \cdot \dot{u}\,(t) \cdot du \tag{14}$$

The integral in equation 14 does not have a trivial solution because the function present 6 discontinuities corresponding to the *F*-*u* corner points and the law characterising the different damping force depends on the displacement level achieved by the system. Adopting a similar approach, Giannini and Masiani [23] assuming a sine wave displacement rocking response for a rigid block (bi-linear *F*-*u* relationship), derived the following equivalence:

$$\xi = \frac{2 \cdot (1 - e)}{\pi \cdot (1 + e)} \tag{15}$$

Therefore, the work will be focused in studying the relationship between these two quantities for the presented viscous damping models and *F-u* relationship introduced.

5 IMPLEMENTED SDOF MODEL

The numerical model adopts the Newmark 'linear acceleration method' [24] integration scheme implemented in the non-iterative formulation version. It solves the SDOF equation introduced in equation 6 substituting the rigid bi-linear system restoring force $f_{bi}\,(u(t))$ with the tri-linear curve $f_{tri}\,(u(t))$ discussed in section 3. The implemented damped SDOF equation of motion in the three damping configurations studied follows:

$$m_{eff} \cdot \ddot{u}(t) + \begin{matrix} C_{CDC} \\ C_{CDR}(t) \\ C_{SDR}(t) \end{matrix} \cdot \dot{u}(t) + f_{tri}\,(u(t)) = -\lambda \cdot m_{eff} \cdot \ddot{u}_g(t) \tag{16}$$

The SDOF model adopting the coefficient of restitution lacks at the damping force terms reducing the system velocity by means of equation 8. In order to validate the numerical model Figure 4a shows the comparison between damped free vibration responses obtained with the implemented SDOF model and the SDOF proposed by Sorrentino *et al.* [5].

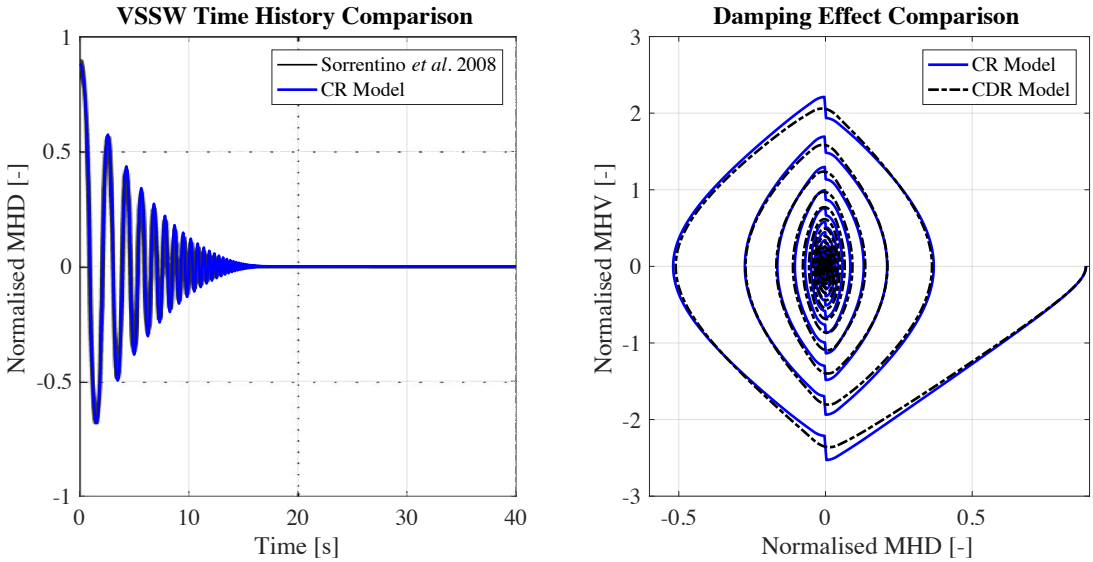

Figure 4: Left side: comparison between damped free vibration response time histories of a VSSW obtained by the presented SDOF and by Sorrentino *et al*. [5]. Details of the wall: t=0.4 m, h=4.0 m, O=0 N, u_0=0.9· u_{ins}, $\dot{u}_0$=0, $\ddot{u}_0$=0, e= e_{an}=0.955 (equation 7). Right side: comparison between matched damped free vibration responses in terms of normalised MHD and normalised MHV of a VSSW obtained by adopting the coefficient of restitution and a CDR model.

Figure 4b proposes instead a comparison between matched free vibration responses in terms of normalised mid-height displacement (MHD) and normalised velocity (MHV) obtained by adopting the coefficient of restitution CR and a constant damping ratio CDR model. It is worth noticing as in the impact region whereas the coefficient of restitution acts, reducing suddenly the system velocity, the CDR model decreases smoothly the velocity without inducing a clear discontinuity on it but acting at the same time similarly to a coefficient of restitution model.

6 DERIVATION OF THE EQUIVALENCE

The work consisted in analysing the damped free vibration response provided by the different damping systems and comparing them. The coefficient of restitution model has been taken as the reference damping systems. In order to ensure the equivalence between the energy dissipation provided by the different systems, satisfying the equivalence between equation 13 and 14, the damped free vibration decays provided by a velocity dependent acting force (CDC, CDR, SDR) have been matched with the ones provided by a SDOF adopting a coefficient of restitution. An error has been defined in order to proper select the damping ratio value that allowed to minimise the difference with the coefficient of restitution response for each system.

$$Err = \sum_{j=1}^{k} (|u_{CR}(j)| - |u_{DAF}(j)|)^2 \tag{17}$$

Err represents the summation of absolute difference between the coefficient of restitution decay and the one provided by the models with a damping acting force (CDC, CDR, SDR) at each analysis time step for the entire length of the response (k).
Figure 5 plots the damping ratio values corresponding to each model that minimised the error for a specific VSSW and a defined set of coefficients of restitution. It is also shown the effect of the amplitude of oscillation releasing the VSSW from an initial imposed displacement equal to 0.9, 0.5 and 0.3 times the instability displacement. In general, all the models present a higher dispersion moving towards higher coefficients of restitution. The equivalence related to the CDC Model is the most sensitive to the oscillation amplitude while the CDR Model is only slightly affected by this variable. In both CDC and CDR models damped high oscillation amplitudes are associated to lower damping ratio values, while for the SDR Model the trend is reversed: slightly higher damping ratio values are associated to higher oscillations. This is associated to the nature of the SDR Model which tend to associate very low damping ratio values to oscillations close to collapse, consequently the request initial damping value to fit the response given by a CR Model is slightly higher.

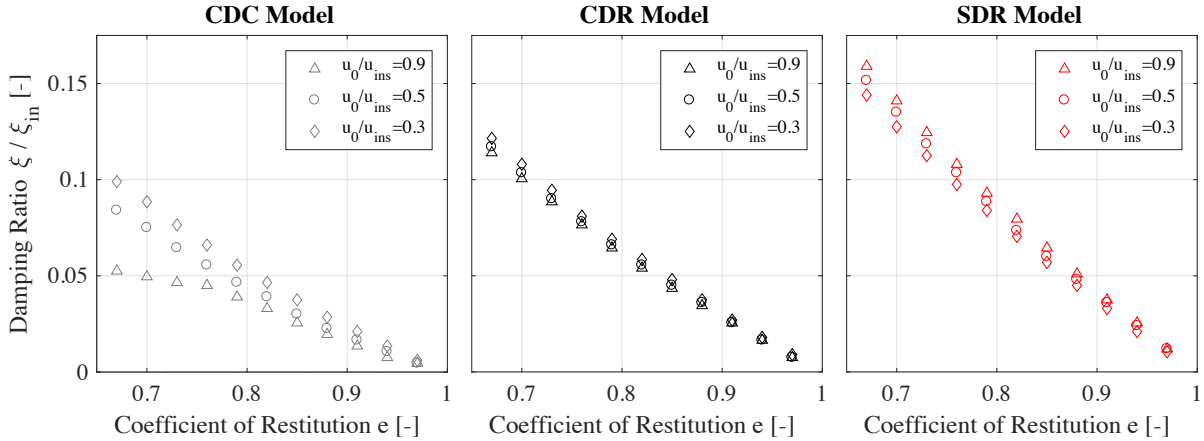

Figure 5: Comparison between CDC, CDR and SDR models in matching free vibration responses damped by a coefficient of restitution model. Details of the VSSW adopted for the comparison: a_1=0.04, b_1=0.85, a_3=1, O=0, h_1/h=0.7, t=0.3 and λ=15.

This finding confirm as a CDC model is not a good choose in simulating the energy dissipation involved in rocking mechanism. For the following comparisons, the authors considered as reference starting oscillation amplitude 0.5 the instability displacement. Figure 6 (top and centre rows) illustrates as the equivalence, once defined a specific tri-linear configuration in terms of

a_1, a_3 and b_1, is independent from the system slenderness and the acting axial load for all the damping models presented. On the contrary, the damping ratio values matching the coefficient of restitution response are affected by the chosen tri-linear a_1 parameter which controls the initial cracked stiffness (see Figure 6 bottom). Again, the most sensitive model to a_1 variations is the CDC one while the less affected is the CDR model. A higher initial stiffness leads to lower values of damping ratio for both CDC and CDR models, the SDR, instead, associates lower damping ratio values to lower a_1 parameters.

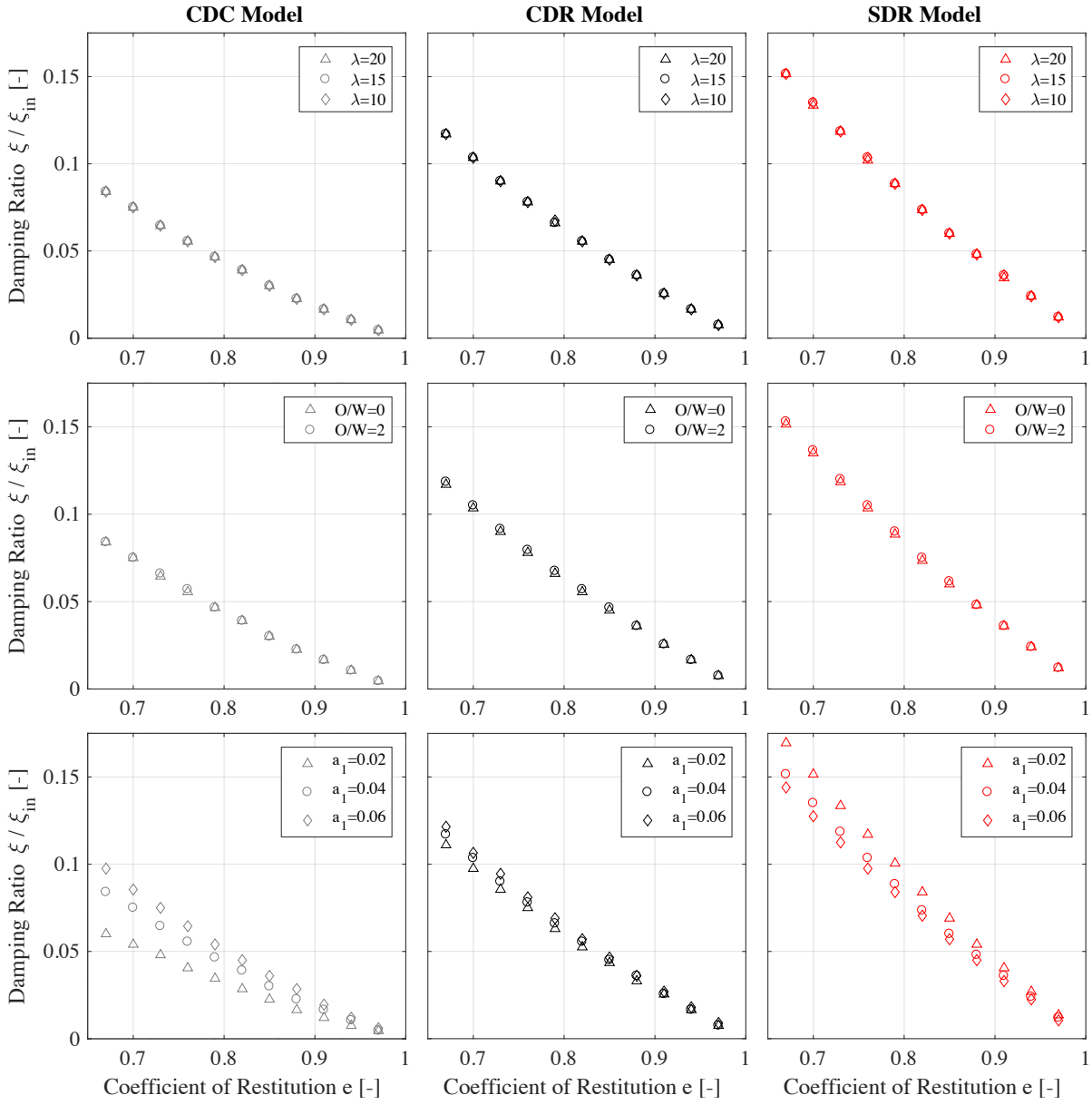

Figure 5: Comparison between CDC, CDR and SDR models in matching free vibration responses damped by a coefficient of restitution model. Details of the VSSW in the top row: a_1=0.04, b_1=0.85, a_3=1, O=0, h_1/h=0 and t=0.3. Details of the VSSW centre row: a_1=0.04, b_1=0.85, a_3=1, h_1/h=0, t=0.3 and λ=15. Details of the VSSW in the bottom row: b_1=0.85, a_3=1, h_1/h=0.7, O=0, t=0.3 and λ=15.

This is particularly evident for low values of e that, causing a drop of the oscillation amplitudes, tends to concentrate the free vibration response in low amplitude oscillations, greatly

affected by a_1; the lower a_1 the quicker the oscillations decay and the higher the requested SDR damping.

Figure 6 plots the minimum errors defined in equation 17 associated to the best fit considering a specific VSSW configuration. The errors have been displaced in root due to their wide variation with coefficient of restitution: the lower e the higher Err is. Both damping models acting on the secant stiffness (CDR and SDR) presented lower errors compared to the CDC model. The CDR presented the lowest errors in matching free vibration decays controlled by the coefficient of restitution in a range of e values between 0.91 and 0.8; the remaining coefficient of restitution decays have been simulated more efficaciously by a SDR model.

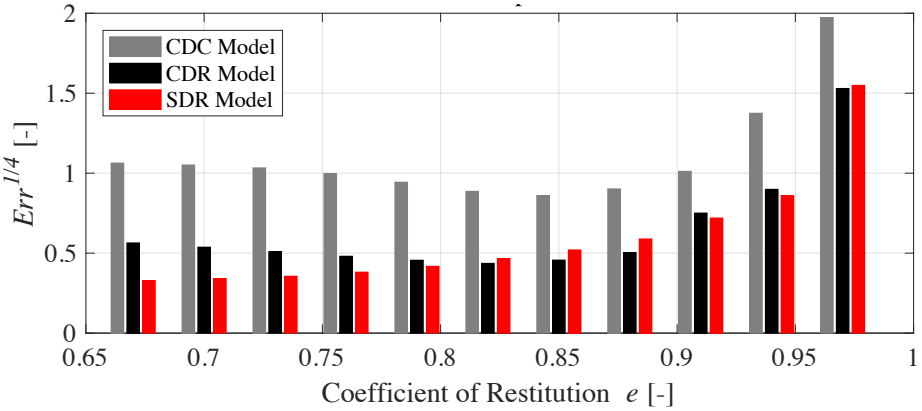

Figure 6: Comparison between errors associated to CDC, CDR and SDR models in matching free vibration responses damped by a CR. Details of the VSSW: a_1=0.04, b_1=0.85, a_3=1, O=0, h_1/h=0.7, t=0.3 and λ=15.

7 EXPERIMENTAL VALIDATION OF THE PROPOSED EQUIVALENCE

The results previously shown suggested that the cracked stiffness (controlled by parameter a_1) is the system characteristic that more affects the equivalence between velocity dependent acting force models and the coefficient of restitution. Figure 7 shows a second order polynomial fit of this dependence for each model compared to the one proposed by Giannini and Masiani [23]. CDC and SDR give damping ratio values lower and higher respectively than the ones provided by equation 15. The CDR model, instead, seems rather close to the equivalence proposed by Giannini and Masiani, with only slightly lower values and a reduced dependence on a_1.

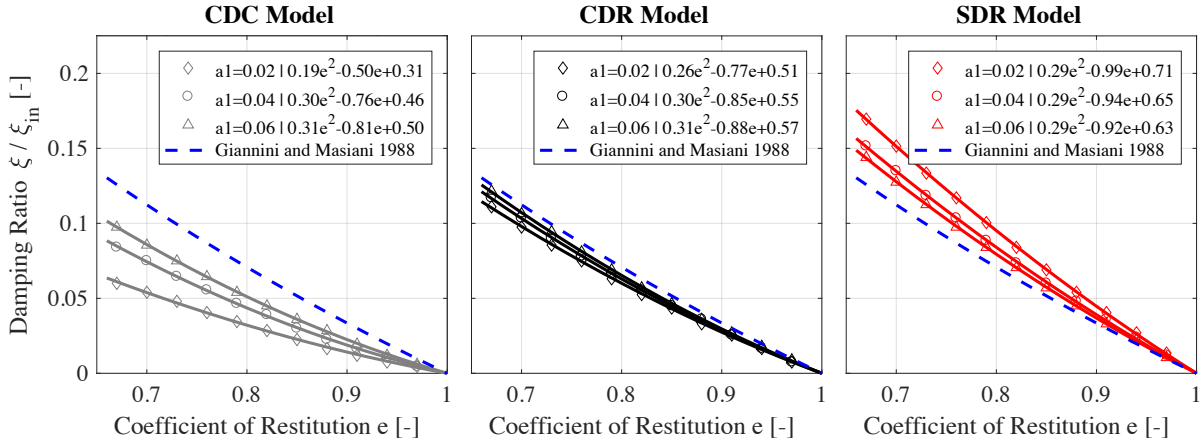

Figure 7: Comparison between proposed 2nd order polynomial fits and the relationship proposed by Giannini and Masiani [23]. Details of the VSSW: b_1=0.85, a_3=1, h_1/h=0.7, O=0, t=0.3 and λ=15.

In order to ensure the reliability of the proposed equivalence, a comparison between the performance of the different damping systems in simulating a dynamic OOP experimental response the is proposed. The reference experimental campaign is the one performed by Graziotti *et al.* and Tomassetti *et al.* [17, 25] consisting in series of shaking table tests on URM single leaf and cavity walls subjected to a pure OOP one-way bending action. Among the different signals a test performed adopting a 2 Hz Ricker Wave Acceleration input on the 0.3MPa-vertical-loaded specimen (i.e. SIN-03-00, test #2.4) has been selected for the comparison. It consisted of a particular acceleration pulse that induced a clear damped free vibration phase in the specimen, providing valuable information on the damping forces acting on the specimens. First of all, the experimental response has been calibrated selecting a reasonable tri-linear configuration and a coefficient of restitution equal to 0.835 close to the average value of 0.852 measured experimentally from peak response velocity ratio values [17]. The damping ratio values associated to each damping model have been calculated by averaging the values obtained by the equations in Figure 7 for a_1 values of 0.2 and 0.4 (having assumed to model the experimental response an a_1 value of 0.3). Figure 8 shows the comparison between experimental and numerical MHD histories.

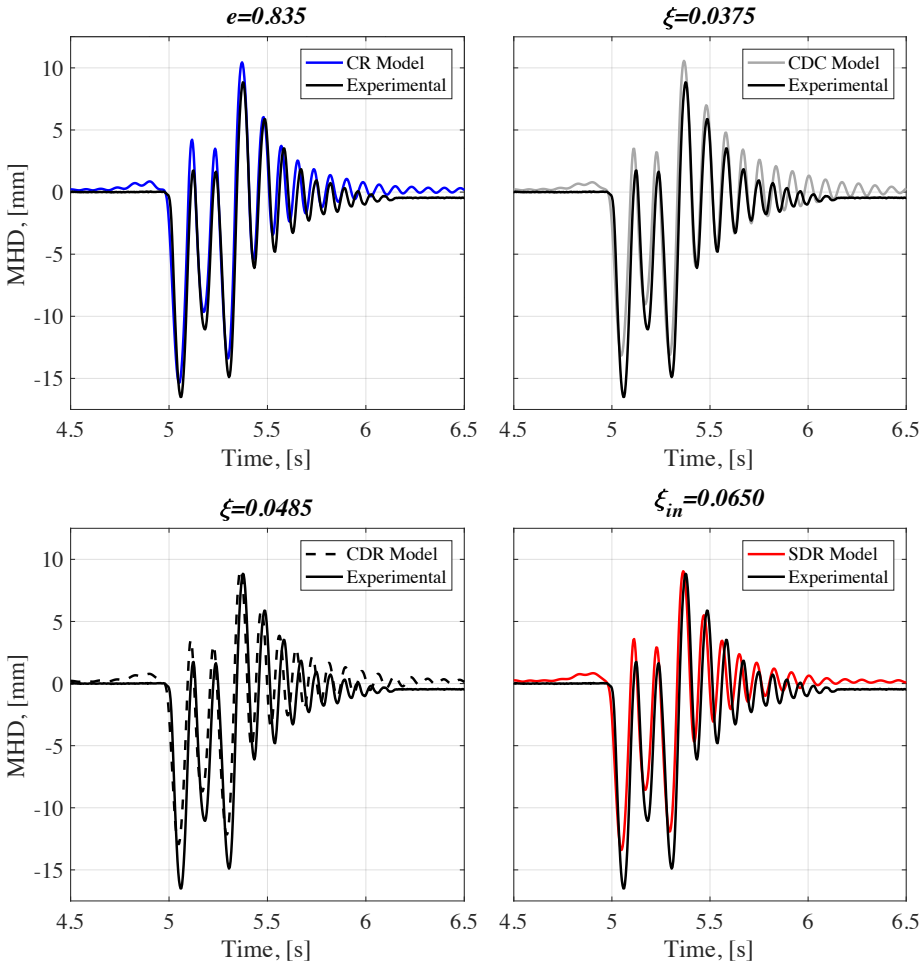

Figure 8: Comparison between numerical and experimental MHD histories of the different damping models. Details of the parameters necessary to simulate the SIN-03-00 response: a_1=0.03, b_1=0.80, a_3=1, O/W=6.2, h_1/h=0.57, t=0.102 and λ=27.

The SDR seems to damp the system slightly more than the other models. As the oscillation amplitude is lower (reduced u_p/u_{ins}), the SDR and the CDR tend to damp the system much more similarly each other due to the reduced contribution of the secant stiffness region. For this reason, low amplitudes test may slightly be overdamped if the polynomial fit presented in Figure 7, which has been derived for larger oscillation amplitudes (0.5 u_p/u_{ins}), is used. This is one of the shortcoming of adopting a SDR Model that, on the other hand, resulted the most effective in simulating the amplitude of response peaks during the decay.

8 CONCLUSIONS

The paper presents a simplified SDOF model for the evaluation of the out-of-plane one-way-bending dynamic response of URM walls. The model consists of a trilinear nonlinear elastic oscillator that could be associated with different damping models: coefficient of restitution, constant damping coefficient, constant damping ratio and stiffness proportional damping ratio both acting on the secant stiffness. The systems were calibrated against experimental results (procedure not reported in this work).

The final goal of the work was to define relationships between these numerical damping techniques. The coefficient of restitution model has been taken as the reference damping systems. In order to ensure the equivalence between the energy dissipation provided by the systems, the different damped free vibration decays have been matched with the ones provided by a SDOF model analyses adopting a coefficient of restitution.

Polynomial relationships were provided in order to directly correlate the different damping models with the coefficient of restitution. In general, these equivalences depend on the amplitude of oscillation and the relative initial stiffness of the systems. They were found to be substantially not dependent on the system slenderness and on the acting vertical overburden force. The constant damping ratio (CDR) model acting on the system secant stiffness, also considering its reduced dependence on oscillation amplitude and initial stiffness, resulted the most appropriate in simulating free vibration decays damped by a coefficient of restitution. In addition, the stiffness proportional damping ratio (SDR) model has shown rather good performances.

A further extension of the present work will be the validation of the proposed equivalences comparing the results of the different models subjected to a large sets of natural ground motions or more in general forced vibrations.

REFERENCES

[1] A. Giuffrè, A mechanical model for statics and dynamics of historical masonry buildings. *Protection of the Architectural Heritage Against Earthquakes*, Springer-Verlag: Wien, 71-152, 1996.

[2] D. Dizhur, J. Ingham, L. Moon, M.C. Griffith, A. Schultz, I. Senaldi, G. Magenes, J. Dickie, S. Lissel, J. Centeno, C. Ventura, J. Leite, P. Lourenco. Performance of masonry buildings and churches in the 22 February 2011 Christchurch earthquake. *Bull. New Zealand Society for Earthquake Engineering,* **44**(4):279-296, 2011

[3] J. Ingham, M.C. Griffith, Performance of unreinforced masonry buildings during the 2010 Darfield (Christchurch, NZ) earthquake. *Australian Journal of Structural Engineering*., **11**(3): 207-224, 2011.

[4] G.W. Housner, The behavior of inverted pendulum structures during earthquakes. *Bull. Seismological Society of America*, **53**(2): 403–417, 1963.

[5] L. Sorrentino, R. Masiani, M.C. Griffith, The vertical spanning strip wall as a coupled rocking rigid body assembly, *Structural Engineering and Mechanics*, **29**: 433–453, 2008.

[6] K.T. Doherty, An investigation of the weak links in the seismic load path of unreinforced masonry buildings, PhD Thesis, University of Adelaide, Australia, 2000.

[7] M.J. DeJong, E.G. Dimitrakopoulos, Dynamically equivalent rocking structures, *Earthquake Engineering & Structural Dynamics*, **43**(10): 1543–1563, 2014.

[8] L.F. Restrepo Vélez, Seismic risk of unreinforced masonry buildings. PhD thesis, ROSE School, University of Pavia, Italy, 2004.

[9] N. Makris, D. Konstantinidis, The rocking spectrum and the limitations of practical design methodologies. *Earthquake Engineering & Structural Dynamics*, **32**(2):265–89, 2003.

[10] M.C. Griffith, G. Magenes, G. Melis, L. Picchi, Evaluation of out-of-plane stability of unreinforced masonry walls subjected to seismic excitation. *Journal of Earthquake Engineering*, **7**,141-169, 2003

[11] S. Lagomarsino, Seismic assessment of rocking masonry structures, *Bulletin of Earthquake Engineering*, **13**:97-128, 2014.

[12] T.M. Ferreira, A.A. Costa, R. Vicente, H. Varum, A simplified four-branch model for the analytical study of the out-of-plane performance of regular stone URM walls, *Engineering Structures*, **83**,140–153, 2015.

[13] N.T.K. Lam, M.C. Griffith, J. Wilson, K.T. Doherty, Time-history analysis of URM walls in out-of-plane flexure. *Engineering Structures*, **25**(6):743–754, 2003.

[14] U. Tomassetti, F. Graziotti, A. Penna, G. Magenes, A Single-Degree of Freedom Model for the Simulation of the Out-of-Plane Response of Unreinforced Masonry Walls, *Proc. 16th Italian Conf. on Earthquake Engineering*, L'Aquila, Italy, 2015.

[15] H. Derakhshan, D.Y. Dizhur, M.C. Griffith, J.M. Ingham, Seismic Assessment of out-of-plane loaded unreinforced masonry walls in multi-storey buildings, *Bulletin of New Zealand Society for Earthquake Engineering*, **47**(2): 119-138, 2014.

[16] ABK. Methodology for Mitigation of seismic hazards in existing unreinforced masonry buildings: wall testing, out of plane. *Topical Report 04*, c/o Agbabian Associates, El Segundo, California; 1981.

[17] F. Graziotti, U. Tomassetti, A. Penna, G. Magenes, Out-of-plane shaking table tests on URM single leaf and cavity walls, *Engineering Structures*, **125**, 455-470, 2016

[18] H. Derakhshan, M.C. Griffith, J.M. Ingham, Airbag testing of multi-leaf unreinforced masonry walls subjected to one-way bending. *Engineering Structures* **57**, 512-522, 2013

[19] H. Derakhshan, M.C. Griffith, J.M. Ingham, Out-of-plane behaviour one-way spanning unreinforced masonry walls. *Journal of Engineering Mechanics,* **139**(4): 409-417. 2013

[20] L. Sorrentino, O.A. Shawa, L.D. Decanini, The relevance of energy damping in unreinforced masonry rocking mechanisms. Experimental and analytic investigations. *Bulletin of Earthquake Engineering*, **9**(5):1617-1642, 2011.

[21] M. Aslam, W. Godden, D. Scalise, Rocking and overturning response of rigid bodies to earthquake motions. *Report University of California*, Berkeley, LBL-7539 UC-11, 1978.

[22] L. Sorrentino, Dinamica di muri sollecitati fuori del piano come sistemi di corpi rigidi. PhD thesis, Sapienza University of Rome, Italy, (in Italian), 2003.

[23] R. Giannini, R. Masiani, Dinamica delle oscillazioni dei blocchi rigidi, *IX Congresso nazionale dell'associazione italiana di meccanica teorica ed applicate*, (in Italian), 1988.

[24] N. M. Newmark, A method of computation for structural dynamics. *Journal of Engineering Mechanics*, ASCE, **85** (EM3) 67-94, 1959.

[25] U. Tomassetti, F. Graziotti, A. Penna, G. Magenes, Out-of-Plane Shaking Table Test on Unreinforced Cavity Walls. *Proceedings of 16th International Brick/Block Masonry Conference (IBMAC)*, Padua, Italy, 2016.